

Photoinduced Electron Transfer in Ethidium-Modified DNA Duplexes: Dependence on Distance and Base Stacking

Shana O. Kelley, R. Erik Holmlin, Eric D. A. Stemp,[†] and Jacqueline K. Barton*

Contribution from the Beckman Institute, Division of Chemistry and Chemical Engineering, California Institute of Technology, Pasadena, California 91125

Received May 6, 1997[⊗]

Abstract: Long-range photoinduced electron transfer has been systematically examined in a series of small DNA duplexes covalently modified with ethidium and Rh(phi)₂bpy³⁺ through time-resolved and steady-state measurements of fluorescence quenching. Fast fluorescence quenching ($k \geq 10^{10} \text{ s}^{-1}$) is observed for this donor/acceptor pair noncovalently bound to DNA, and transient absorption studies allow the assignment of this quenching to an electron-transfer mechanism. In the duplexes modified with tethered intercalators, intrahelix fluorescence quenching attributed to electron transfer occurs at distances up to 30 Å. Over a donor/acceptor separation of ~ 20 Å, approximately 30% of the ethidium fluorescence is quenched, while at a separation of ~ 30 Å, approximately 10% quenching is observed. Time-resolved measurements indicate that this quenching is primarily static. Fluorescence polarization and melting studies indicate that the intercalators are rigidly bound, enhance helix stability, and the duplex populations are structurally homogeneous. The distance dependence of the quenching yield observed in these duplexes is shallow, but the quenching reaction is highly sensitive to stacking perturbations. Changes in the quenching yield with melting are directly correlated with hypochromicity associated with base stacking. Moreover, in duplexes containing a highly disruptive CA mismatch, large decreases in the quenching efficiency are observed, while with a well-stacked GA mismatch, electron transfer proceeds efficiently. Hence, in these covalently-modified assemblies, DNA-mediated electron transfer is found to depend only weakly on donor/acceptor separation, when compared to protein systems, but is highly sensitive to perturbations in base stacking.

Introduction

For more than 30 years, both experiment^{1–22} and theory^{23–29} have been applied to determine whether the DNA π -stack facilitates charge transport over extended molecular distances. The dynamics and distance dependence of charge transfer through DNA may have important consequences for DNA damage and repair mechanisms, as many nucleic acid lesions are the result of redox processes. The recent discoveries of oxidative damage to DNA¹ and the oxidative repair of thymine dimers² in DNA over distances greater than 30 Å now underscore implications for long-range charge transport within the cell.

In order to investigate DNA as an electron-transfer medium, spectroscopic studies have focused on DNA-bound donor/acceptor pairs;^{3–14} these studies have produced seemingly conflicting results. In studies of electron transfer between ethidium (Et), an intercalator, and *N,N'*-dimethyl-2,7-diazapyrenium dichloride (DAP), a molecule which may either intercalate or groove bind, the rate of electron-transfer was found to $\leq 10^9 \text{ s}^{-1}$, and it was suggested that electronic coupling through DNA was protein-like ($\beta = 1 \text{ Å}^{-1}$), based upon estimated distances.¹⁰ Ultrafast spectroscopy applied to studies of metallointercalators noncovalently bound to DNA with dilute loadings (1 (donor/acceptor)/50 bp) revealed fast photoinduced

electron transfer (10^{10} s^{-1}),⁴ suggesting a shallow distance dependence compared to proteins. These fast electron-transfer kinetics have also been interpreted within the context of a cooperative clustering model.^{4,30,31} However, studies across a wide array of donor/acceptor pairs and different DNA sequences has not been described by a clustering model. These studies all underscore the need to use covalently bound donors and acceptors to evaluate unambiguously the distance dependence of electron transfer in DNA.

Few studies of photoinduced electron transfer with DNA as a bridge intervening between covalently bound reactants have been conducted, and these investigations have produced intriguing results.^{3,14,15} In a DNA duplex modified with an intercalating Ru(II)/Rh(III) pair, subnanosecond luminescence quenching occurred at a distance of 41 Å.³ In a different study utilizing a shorter duplex modified with nonintercalating reactants, significantly slower electron transfer was found.¹⁴ Most recently, the distance dependence of electron transfer through DNA was studied for a stilbene-derivatized hairpin.¹⁵ From the results of this study, DNA was determined to be a more efficient medium for electron transfer than proteins, but a steeper distance dependence was observed than was indicated by the first study employing intercalated reactants. The disparity between the results of these studies may be a consequence of the different donor–DNA–acceptor linkages used in these systems which certainly influence the interaction between the reactants and DNA. The most efficient electron-transfer reaction

* To whom correspondence should be addressed.

[†] Present address: Mt. St. Mary's College, Los Angeles, CA 90049.

[⊗] Abstract published in *Advance ACS Abstracts*, October 1, 1997.

(1) Hall, D. B.; Holmlin, R. E.; Barton, J. K. *Nature* **1996**, 382, 731.

(2) Dandliker, P. J.; Holmlin, R. E.; Barton, J. K. *Science* **1997**, 275, 1465.

(3) Murphy, C. J.; Arkin, M. A.; Jenkins, Y.; Ghatlia, N. D.; Bossman, S.; Turro, N. J.; Barton, J. K. *Science* **1993**, 262, 1025.

(4) Arkin, M. R.; Stemp, E. D. A.; Holmlin, R. E.; Barton, J. K.; Hörmann, A.; Olson, E. J. C.; Barbara, P. A. *Science* **1996**, 273, 475.

(5) Barton, J. K.; Kumar, C. V.; Turro, N. J. *J. Am. Chem. Soc.* **1986**, 108, 6391.

(6) Purugganan, D.; Kumar, C. V.; Turro, N. J.; Barton, J. K. *Science* **1986**, 241, 1645.

(7) Murphy, C. J.; Arkin, M. A.; Ghatlia, N. D.; Bossman, S.; Turro, N. J.; Barton, J. K. *Proc. Natl. Acad. Sci. U.S.A.* **1994**, 91, 5315.

(8) Arkin, M. R.; Stemp, E. D. A.; Turro, C.; Turro, N.; Barton, J. K. *J. Am. Chem. Soc.* **1996**, 118, 2267.

(9) Holmlin, R. E.; Stemp, E. D. A.; Barton, J. K. *J. Am. Chem. Soc.* **1996**, 118, 5236.

featured intercalated donors and acceptors, which allow intimate association with the stacked bases, while in the systems where the direct coupling of donors and acceptors into the π -stack may have been diminished through nonintercalative connectivities, steeper distance dependences and slower kinetics were exhibited.

Here, for the first time, photoinduced electron transfer between intercalators covalently bound to DNA is examined as a function of distance and base stacking. The donor employed, ethidium, is a classical intercalator ($K \sim 10^6 \text{ M}^{-1}$),^{32,33} and the acceptor is Rh(phi)₂bpy³⁺ (phi = 9,10-diimine phenanthrenequinone), a metallointercalator ($K \geq 10^6 \text{ M}^{-1}$).³⁴ Both of these molecules have been functionalized with methylene tethers and attached to DNA duplexes 10–14 base pairs in length. We find that fluorescence quenching occurs by electron transfer over distances ranging from 17–36 Å. Although this DNA-mediated electron-transfer reaction is weakly dependent on distance, it depends sensitively upon base stacking. Indeed, with perturbations in stacking, large decreases in the quenching efficiency are observed. Our findings support the notion that the DNA base stack facilitates direct long-range electron transfer.

Experimental Section

Synthesis and Characterization. Unless otherwise noted, all reagents and starting materials used in synthetic protocols were purchased from Aldrich or Fluka and used without further purification. Reagents for oligonucleotide synthesis were obtained from Glen Research. [Rh(phi)₂bpy]Cl₃ was prepared, and the enantiomers of this complex were resolved as previously described.³⁴

Synthesis of *N*-Glycyl Ethidium (Et'). Ethidium bromide (1 equiv, 1 g) was heated at 70 °C in a small volume of DMF (~50 mL) with glutaric anhydride (1 equiv) for 48 h. The solvent was removed *via* rotary evaporation, and the residue dissolved in H₂O/CH₃CN. Starting material and the disubstituted product were separated from the desired monosubstituted form on a cation (Sephadex C-25) exchange column. The crude mixture was loaded on the column, the yellow disubstituted product was eluted at neutral pH, and the orange-pink monosubstituted product was eluted upon raising the pH of the mobile phase. This material contains both the 3'- and 8'-functionalized isomers, although mainly the desired 8' form, hence the isomer mixture was used directly in conjugate synthesis. Identity of the product was confirmed using FAB mass spec (calc. (found) m/z (M^+) = 428 (428)), ¹H NMR (300 MHz, CD₃OD), δ (ppm): 1.45 (m, 3H, N5-CH₃), 2.0–2.4 (m, 6H, side chain CH₂), 4.7 (2H, N5-CH₂), 7.4 (m, 2H: H₂, H₄), 7.6–7.8 (m,

6H: ϕ H, H₉), 8.6 (m, 2H: H₁, H₁₀), and ultraviolet-visible (UV-vis) absorption spectroscopy ($\lambda_{\text{max}}(\text{vis}) = 460 \text{ nm}$, $\epsilon = 5.7 \times 10^3 \text{ M}^{-1} \text{ cm}^{-1}$).

Modification of Oligonucleotides. Unmodified oligonucleotides were prepared using standard automated techniques³⁵ on a 394 ABI synthesizer and purified by reversed phase HPLC. For conjugate synthesis, oligonucleotides lacking the terminal 5'-dimethoxytrityl group were synthesized on a 2000 Å controlled pore glass (CPG) support. A diamiononane linker was attached to the oligonucleotide on the resin using procedures previously described.³⁶

To effect coupling with amino-terminated oligonucleotides, the succinimidyl ester of Et' was first prepared *in situ* by combining Et' in 1:1:1 CH₂Cl₂/DMF/dioxane with 10 equiv of *N,N'*-disuccinimidyl carbonate for 15 min or alternatively by stirring Et' with 10 equiv of *O*-(*N*-succinimidyl)-*N,N,N',N'*-tetramethyluronium tetrafluoroborate (TSTU) in 1:1:1 CH₃CN/CH₃OH/CH₂Cl₂ and 5 equiv of diisopropylethylamine for 30 min. Once activation was confirmed *via* thin layer chromatography (alumina/MeOH, R_f Et'-NHS \gg Et'), the amino-derivatized DNA on the CPG support was added to the Et' solution, and the mixture was stirred overnight at ambient temperature. The Et'-DNA-CPG was isolated from the reaction mixture by vacuum filtration and washed with H₂O, CH₃CN, and a small amount of CH₃OH. The Et'-DNA was then cleaved from the resin, and the protecting groups on the oligonucleotide removed by incubating at 55 °C in concentrated (30%) NH₄OH overnight. The NH₄OH solution was subsequently evaporated and the modified oligonucleotides purified in the same manner as unmodified oligonucleotides using reversed phase HPLC. For a gradient of 50 mM ammonium acetate/CH₃CN increasing from 0% to 40% CH₃CN over 40 min on a C4 column, the modified conjugates have a retention time of ~30 min, while underivatized DNA elutes with a retention time ~15 min. The product is identified by a characteristic DNA/Et' hybrid spectrum ($\lambda_{\text{max}} = 260 \text{ nm}$, 484 nm). Rhodium-modified oligonucleotides were prepared in an analogous manner as previously described;¹ diastereomeric Δ -Rh and Λ -Rh-containing conjugates were resolved using reversed phase HPLC. Quantitation of Et- and Rh-modified conjugates was performed using extinction coefficients of $\epsilon_{(\text{Et}, 484)} = 4.0 \times 10^3 \text{ M}^{-1} \text{ cm}^{-1}$ and $\epsilon_{(\text{Rh}, 390)} = 19.5 \times 10^3 \text{ M}^{-1} \text{ cm}^{-1}$, which were evaluated from phosphate analysis³⁷ and other stoichiometry determinations.

The conjugates have also been characterized by matrix-assisted time-of-flight (MALDI-TOF) and electrospray ionization mass spectrometry and base analysis by enzymatic digestion.³⁸ In the case of Et'-5'CTATCTATCGT, the 11 base conjugate used in this study, the mass of the conjugate was obtained by MALDI-TOF mass spectrometry (calc. (found) m/z ($\text{M}(-\text{H})$) 3877 (3874 \pm 5)). All other masses of Et-modified sequences obtained by MALDI-TOF were within 3 m/z of calculated values. Characterization of rhodium-modified oligonucleotides will be described elsewhere.³⁹ The base ratios obtained by digestion followed by quantitation *via* HPLC for this conjugate were as follows: dC = 3.03, dG = 0.96, dT = 4.07, dA = 2.03, dT + Et'-linker = 1.0.

Hybridization of DNA Duplexes. Based on the extinction coefficients listed above for modified conjugates and calculated extinction coefficients for unmodified sequences ($\epsilon_{260} (\text{M}^{-1} \text{ cm}^{-1})$): dC = 7.4×10^3 ; dG = 12.3×10^3 ; dT = 6.7×10^3 ; dA = 15.0×10^3), appropriate amounts of complementary materials were combined at 1:1 stoichiometry and dissolved in 5 mM phosphate, 50 mM NaCl (pH 7) to give a final duplex concentration of 5 μM . The resulting solutions were heated to 90 °C and slowly cooled to ambient temperature over 2–3 h to anneal the duplex.

Melting Profiles. Thermal denaturation experiments were performed on a HP8452A diode array spectrophotometer with samples at a duplex

- (10) Brun, A. M.; Harriman, A. *J. Am. Chem. Soc.* **1992**, *114*, 3656.
 (11) Baguley, B. C.; LeBret, M. *Biochemistry* **1994**, *23*, 937.
 (12) Davis, L. M.; Harvey, J. D.; Baguley, B. C. *Chem.-Biol. Interactions* **1987**, *62*, 45.
 (13) Fromhertz, P.; Rieger, B. *J. Am. Chem. Soc.* **1986**, *108*, 5361.
 (14) Meade, T. J.; Kayyem, J. F. *Angew. Chem., Int. Ed. Engl.* **1995**, *34*, 352.
 (15) Lewis, F. D.; Wu, Taifeng; Zhang, Y.; Letsinger, R. L.; Greenfield, S. R.; Wasielewski, M. R. *Science* **1997**, in press.
 (16) Snart, R. S. *Biopolymers* **1968**, *6*, 293.
 (17) Hélène, C.; Charlier, M. *Photochem., Photobiol.* **1977**, *25*, 429.
 (18) Vanlith, D.; Eden, J.; Warman, J. M.; Hummel, A. *J. Chem. Soc., Faraday Trans.* **1986**, *82*, 2933.
 (19) Magan, J. D.; Blau, W.; Croke, D. T.; McConnell, D. J.; Kelly, J. M. *Chem. Phys. Lett.* **1987**, *141*, 489.
 (20) Cullis, P. M.; McClymont, J. D.; Symons, M. C. R. *J. Chem. Soc., Faraday Trans.* **1990**, *86*, 591.
 (21) Houee-Levin, C.; Gardes-Albert, M.; Rouscilles, A.; Ferradini, C.; Hickel, B. *Biochemistry* **1991**, *30*, 8216.
 (22) Pezeshk, A.; Symons, M. C. R.; McClymont, J. D. *J. Phys. Chem.* **1996**, *100*, 18562.
 (23) Felts, A. K.; Pollard, W. T.; Freisner, R. A. *J. Phys. Chem.* **1995**, *99*, 2929.
 (24) Risser, S. M.; Beratan, D. N.; Meade, T. J. *J. Am. Chem. Soc.* **1993**, *115*, 2508.
 (25) Priyadarshy, S.; Risser, S. M.; Beratan, D. N. *J. Phys. Chem.* **1996**, *100*, 17678.

- (26) Dee, D.; Baur, M. E. *J. Chem. Phys.* **1974**, *60*, 541.
 (27) Jovanovic, S. V.; Simic, M. G. *J. Phys. Chem.* **1986**, *90*, 974.
 (28) Colson, A.-O.; Besler, B.; Close, D. M.; Sevilla, M. D. *J. Phys. Chem.* **1992**, *96*, 661.
 (29) Sugiyama, H.; Saito, I. *J. Am. Chem. Soc.* **1996**, *118*, 7063.
 (30) Olson, E. J. C.; Hu, D.; Hörmann, A.; Barbara, P. F. *J. Phys. Chem.* **1997**, *101*.
 (31) Lincoln, P.; Tuite, E.; Norden, B. *J. Am. Chem. Soc.* **1997**, *119*, 1454.
 (32) Waring, M. J. *J. Mol. Biol.* **1965**, *13*, 269.
 (33) LePecq, J. B.; Paoletti, C. *J. Mol. Biol.* **1967**, *27*, 87.
 (34) Pyle, A. M.; Chiang, M.; Barton, J. K. *Inorg. Chem.* **1990**, *29*, 4487.
 (35) Beaucage, S. L.; Caruthers, M. H. *Tetrahedron Lett.* **1981**, *23*, 1859.

concentration of 5 μM in 5 mM phosphate, 50 mM NaCl (pH 7). Absorbance at 260 nm was monitored every 2 $^{\circ}\text{C}$ with 3 min equilibration times.

Electrochemical Measurements. Reduction potentials for ethidium and $\text{Rh}(\text{phi})_2\text{bpy}^{3+}$ were measured *via* cyclic voltammetry on a BAS CV-50W potentiostat in 0.1 M TBAH/ CH_3CN . Cyclic voltammetry was carried out at 20 $^{\circ}\text{C}$ with a normal three electrode configuration consisting of a glassy carbon working electrode, saturated calomel reference electrode, and platinum auxiliary electrode. The ethidium excited-state oxidation potential ($E^{\circ}(\text{Et}^{2+}/\text{Et}^{+*})$) was calculated using the expression $E^{\circ}(\text{Et}^{2+}/\text{Et}^{+*}) = E_{\text{oo}} - E^{\circ}(\text{Et}^{2+}/\text{Et}^{\cdot})$. Values of E_{oo} were approximated both by averaging absorption and emission maxima and examining intersection points of absorption and emission spectra. Both methods yielded equivalent results for ethidium. Potentials are reported *vs* NHE.

Photophysical Measurements. Preparation of Samples with Intercalators Noncovalently Bound to DNA. In sample preparation for steady-state and time-resolved fluorescence measurements employing ethidium and $\text{Rh}(\text{phi})_2\text{bpy}^{3+}$ randomly associated with calf thymus (CT) DNA, the following extinction coefficients were employed: $\epsilon_{(\text{Et}, 484)} = 5.7 \times 10^3 \text{ M}^{-1} \text{ cm}^{-1}$, $\epsilon_{(\text{Rh}, 350)} = 23.6 \times 10^3 \text{ M}^{-1} \text{ cm}^{-1}$, $\epsilon_{(\text{CT DNA}, 260)} = 6.6 \times 10^3 \text{ M}^{-1} \text{ cm}^{-1}$ (nucl.). Appropriate quantities of freshly prepared stock solutions were dissolved in 5 mM phosphate, 50 mM NaCl, pH 7.

Steady-State Fluorescence Experiments. Steady-state fluorescence polarization measurements were made at 20 $^{\circ}\text{C}$ unless otherwise specified with excitation at 480 nm on an SLM 8000 spectrofluorimeter equipped with Glan-Thompson calcite prism polarizers arranged in a T-shaped geometry. Fluorescence intensities were measured on the same apparatus; spectra were integrated from 520 to 800 nm. Typically, samples were measured at a duplex concentration of 5 μM in 5 mM phosphate, 50 mM NaCl (pH 7). In variable viscosity experiments, solutions containing sucrose were prepared, and the viscosities determined with a falling ball viscometer. Quenching yields for modified duplexes obtained by steady-state fluorescence measurements were calculated from 2–5 sets of samples from different syntheses of Et/Rh conjugates.

Time-Correlated Single Photon Counting (TCSPC). TCSPC was carried out using facilities described previously⁴⁰ with $\lambda_{\text{exc}} = 335 \text{ nm}$ obtained by doubling the 670 nm fundamental line; data fitting was accomplished using least-squares methods in a commercial software program (Axum). Data sets contained 5000–10 000 counts, except in cases when small time windows were necessary to ensure constant laser power. Steady-state quenching yields obtained with $\lambda_{\text{exc}} = 480 \text{ nm}$ were identical to those observed with $\lambda_{\text{exc}} = 335 \text{ nm}$. Sample conditions and concentrations were identical in time-resolved and steady-state measurements. No photodegradation was observed, as confirmed by UV–visible absorption spectra taken before and after irradiation.

Results

Photoinduced Electron Transfer between Ethidium and $\text{Rh}(\text{phi})_2\text{bpy}^{3+}$. Fluorescence from the ethidium singlet excited state ($E^{\circ}(\text{Et}^{2+}/\text{Et}^{+*}) \sim -0.9 \text{ V}$)⁴¹ is efficiently quenched by $\text{Rh}(\text{phi})_2\text{bpy}^{3+}$ ($E^{\circ}(\text{Rh}(\text{III})/\text{Rh}(\text{II})) = -0.03 \text{ V}$) when both molecules are noncovalently bound to double-stranded DNA *via* intercalation (Figure 1), as measured by time-resolved (TCSPC) and steady-state techniques. In the presence of DNA, the excited state of ethidium decays with $\tau = 23 \text{ ns}$. With the addition of $\Delta\text{-Rh}(\text{phi})_2\text{bpy}^{3+}$, the ethidium fluorescence can be analyzed as a biexponential decay: Et/DNA/2 equiv of $\Delta\text{-Rh}$

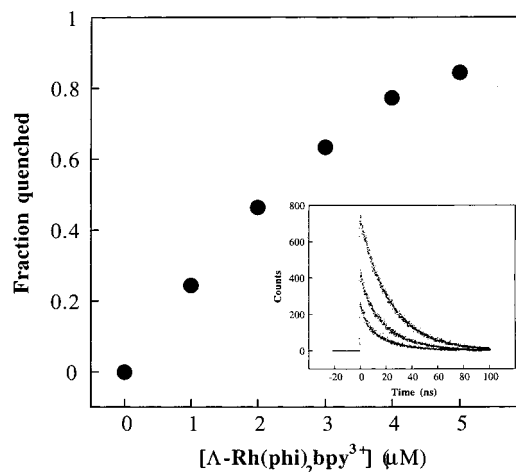


Figure 1. (A) Steady-state fluorescence quenching ($1 - I/I_0$) of ethidium (Et) (10 μM) by $\Delta\text{-Rh}(\text{phi})_2\text{bpy}^{3+}$ (0–50 μM) noncovalently bound to calf thymus DNA (1 mM nucl.), 5 mM phosphate, 50 mM NaCl, pH 7. (B) Excited state decay by TCSPC for 10 μM Et bound to CT DNA (1 mM nucl.) in the absence of acceptor or with 20 and 40 μM $\text{Rh}(\text{phi})_2\text{bpy}^{3+}$.

$\tau_1 = 21 \text{ ns}$ (82%), $\tau_2 = 4.4 \text{ ns}$ (18%); Et/DNA/4 equiv of $\Delta\text{-Rh}$ $t_1 = 19 \text{ ns}$ (68%), $t_2 = 3.5 \text{ ns}$ (32%). Steady-state measurements reveal that in these same samples, the ethidium fluorescence is quenched by 45% in the presence of 2 equiv of the acceptor and by 75% with 4 equiv of the acceptor (Figure 1A).⁴² A small portion of this quenching is reflected in the lifetime changes listed above; however, the majority of the quenching proceeds within the instrument response ($\sim 150 \text{ ps}$) and is reflected in the data shown (Figure 1B) as a decrease in initial intensity. This fast quenching is referred to as static quenching and corresponds to the deactivation of a large portion of the donor molecules on a subnanosecond time scale. While the quenching observed in this system is remarkably efficient, the dependence of the quenching yield on the acceptor loading (17 bp/intercalator (2 equiv), 10 bp/intercalator (4 equiv)) indicates that increasing the number of base pairs between donor and acceptor does decrease the efficiency of electron transfer in this system. Importantly, the observed static quenching cannot correspond to displacement of the donor, as ethidium has a lifetime in water (2.3 ns) which would be detected in this experiment.

Time-resolved transient absorption studies of DNA-bound ethidium and $\text{Rh}(\text{phi})_2\text{bpy}^{3+}$ provide spectroscopic evidence for electron transfer as the quenching mechanism between these two intercalated species. For ethidium bound to calf thymus (CT) DNA in the presence of $\text{Rh}(\text{phi})_2\text{bpy}^{3+}$, long-lived transients consistent with oxidized Et were observed on the microsecond time scale with $\lambda_{\text{max}} = 425 \text{ nm}$.⁴³ In addition, the transient signals were correlated with the amount of quenching observed over a range of acceptor concentrations. These transient absorption data parallel previous studies of metallointercalators where residual recombination on the microsecond time scale was also observed,^{9,44} but measurements using ultrafast spectroscopy showed that the majority of back-electron

(36) Wachter, L.; Jablonski, J. A.; Ramachandran, K. L. *Nucl. Acids Res.* **1986**, *14*, 7985.

(37) Lindberg, O.; Ernsten, L. in *Methods of Biochemical Analysis*; (Glick, D., Ed.); Interscience: New York, 1954; Vol. 3.

(38) Eritja, R.; Horowitz, D. M.; Walker, P. A.; Ziehler-Martin, J. P.; Boosalis, M.S.; Goodman, M. F.; Itakura, K.; Kaplan, B. E. *Nucl. Acids Res.* **1986**, *14*, 8135.

(39) Holmlin, R. E.; Barton, J. K. Manuscript in preparation.

(40) Holmlin, R. E.; Barton, J. K. *Inorg. Chem.* **1995**, *34*, 7.

(41) As the oxidation of ethidium is electrochemically irreversible, this is an upper limit for the excited-state oxidation potential. Lower values have been reported for this potential previously.¹⁰

(42) For intercalated ethidium, $\Delta\text{-Rh}(\text{phi})_2\text{bpy}^{3+}$ is a more efficient quencher than $\Delta\text{-Rh}(\text{phi})_2\text{bpy}^{3+}$ as with 2 equiv of $\Delta\text{-Rh}(\text{phi})_2\text{bpy}^{3+}$ (1 Et/100 bp CT DNA), 30% of the ethidium emission is quenched, while with 4 equiv of $\Delta\text{-Rh}(\text{phi})_2\text{bpy}^{3+}$, 50% quenching is observed. This is a surprising result, because with metallointercalator donors, more efficient electron transfer is typically observed with the $\Delta\text{-Rh}$ enantiomer.⁴ It is possible that the DNA-donor coupling differs in this system such that the enantioselectivity is reversed or that some minor groove binding of the $\Delta\text{-Rh}$ isomer facilitates more diffusional quenching. Due to the larger amount of quenching observed with $\Delta\text{-Rh}(\text{phi})_2\text{bpy}^{3+}$, this isomer was the focus of subsequent studies.

(43) Atherton, S. J.; Beaumont, P. C. *J. Phys. Chem.* **1987**, *91*, 3993.

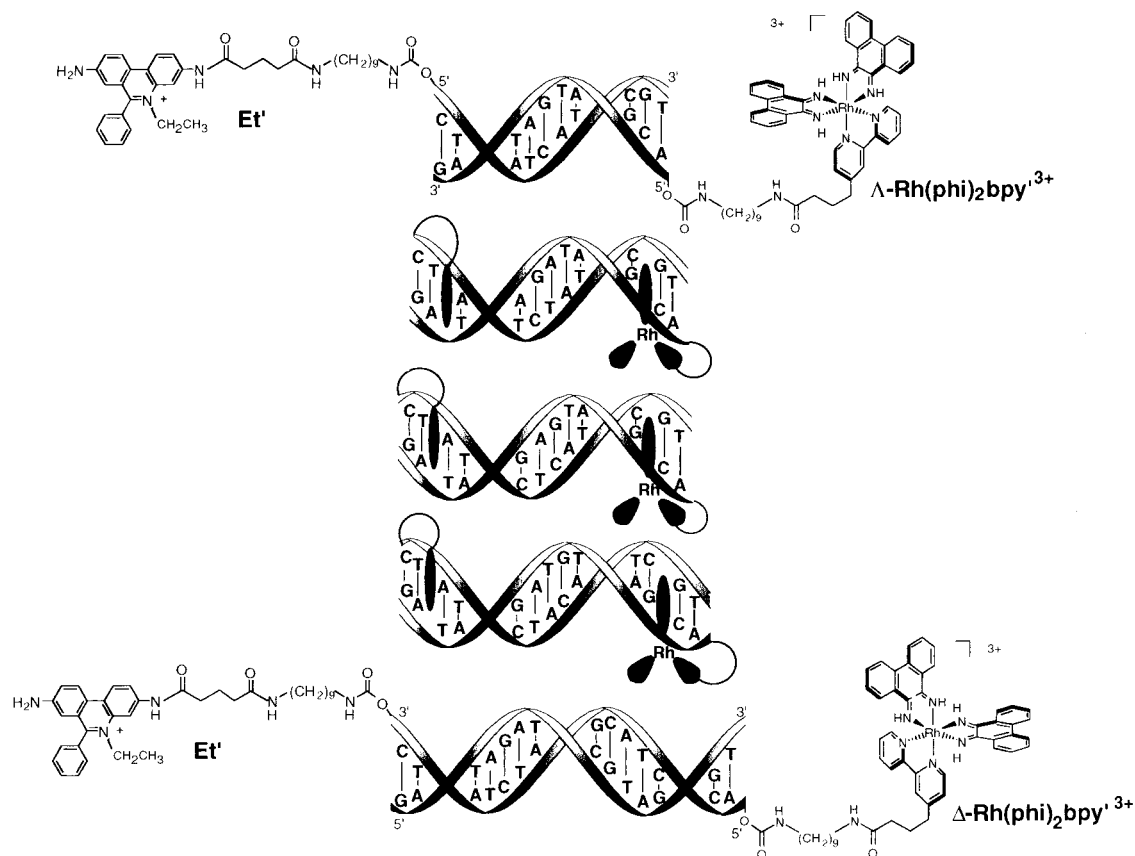


Figure 2. Schematic diagram of the ethidium/rhodium-modified sequences; intercalators and linkers are enlarged here relative to the duplexes for clarity.

transfer occurred on a faster time scale ($k \sim 10^{10} \text{ s}^{-1}$).⁴ For the electron-transfer reaction between ethidium and $\text{Rh}(\text{phi})_2\text{bpy}^{3+}$, the observed transients account for only $\sim 10\%$ of the quenched donors, thus it appears that here too a faster reaction may account for most of the recombination. Given the weak spectroscopic signatures for Et^{2+} and $\text{Rh}(\text{phi})_2\text{bpy}^{2+}$ and the indication that most of the back-electron transfer appears to occur on a very fast time scale, time-resolved transient absorption measurements do not provide a sensitive means to study this reaction. Nevertheless, the correlation between transient yields and quenching yields allows the fluorescence quenching mechanism to be assigned as electron transfer.

The photophysical properties and electron transfer reactivity of *N*-8-glycyl ethidium were also explored, as this derivative of ethidium was most suitable for covalent attachment to DNA. Et' has faster excited-state decay kinetics than the parent molecule; while photoexcited ethidium exhibits a lifetime of 2.7 ns in water, photoexcited Et' decays with a lifetime of 440 ps. Upon intercalation, the emission kinetics of these molecules also differ. In the presence of CT DNA (50 bp/ Et'), ethidium exhibits a monoexponential decay with $\tau = 23$ ns, while the excited state decay for Et' is best described by a biexponential with $\tau_1 = 5.1$ ns (46%), $\tau_2 = 2.3$ ns (54%). Since each of these lifetimes is enhanced compared to the lifetime of Et' free in solution (440 ps), the biexponential decay reflects at least two intercalated geometries rather than a distribution of free and intercalated species. The Et' excited state decay likely contains a distribution of lifetimes reflecting a family of stacking orientations similar to that observed with metallointercalators.^{45–48} Et' bound to DNA undergoes electron transfer to $\text{Rh}(\text{phi})_2\text{bpy}^{3+}$ with the same efficiency as the underivatized donor.

Design and Characterization of Et/Rh-Modified Duplexes.

A series of DNA duplexes, ranging from 10–14 base pairs in length, was synthesized by the 5' modification of amino-nonane terminated oligonucleotides with *N*-8-glycyl ethidium or $\text{Rh}(\text{phi})_2\text{bpy}'^{3+}$ ($\text{bpy}' = 4\text{-butyric acid } 4\text{-methylbipyridine}$) (Figure 2). In varying the length of the ethidium/rhodium(III)-modified (Et/Rh) oligonucleotides, binding sites were conserved, and bases were inserted in the middle of the duplexes. Based on photocleavage experiments, tethered $\text{Rh}(\text{phi})_2\text{bpy}'^{3+}$ is bound predominantly at the second base step for the Λ -Rh-containing diastereomer and equally at the second or third base step for the Δ -Rh-containing diastereomer.¹ As the linker is similar for Et' , we deduce that this intercalator binds at either the second or third base step.⁴⁹ Electron-transfer reactions between covalently bound Et' and modified bases also support the assignment of this binding site.⁵⁰ These binding sites lead to a range of donor–acceptor separations from 17 Å (assuming both intercalators are bound at the third base pair from the respective ends of the 10-mer) to 36 Å (assuming both intercalators are bound at the second base pair from the respective ends of the 14-mer). Distances are therefore listed as ranges in Table 1 reflecting the distribution of possible binding sites, but the variation in donor/acceptor distance with increasing duplex length has a much lower uncertainty; the Et/Rh binding sites are conserved and the linkers are identical across the series of

(44) Stemp, E. D. A.; Arkin, M. R.; Barton, J. K. *J. Am. Chem. Soc.* **1995**, *117*, 2375.

(45) Jenkins, Y.; Friedman, A. E.; Turro, N. J.; Barton, J. K. *Biochemistry* **1992**, *31*, 10809.

(46) Hartshorn, R. M.; Barton, J. K. *J. Am. Chem. Soc.* **1992**, *114*, 5919.

(47) DuPueur, C. M.; Barton, J. K. *J. Am. Chem. Soc.* **1994**, *116*, 10286.

(48) DuPueur, C. M.; Barton, J. K. *Inorg. Chem.* **1997**, *36*, 33.

(49) It is probable that ethidium binds at the second base step, as this tether must extend closer to the base stack due to the planarity of this intercalator.

(50) Kelley, S. O. Unpublished results.

Table 1. Photophysical Data for Et/Rh-Modified Duplexes

sample	length (bp)	D-A sep. ^a (Å)	I_{ss}^b	F_q^c	P^d
Et==	10		0.37		0.185
Et==Λ-Rh	10	17–24	0.26	0.29(2)	0.213
Et==Δ-Rh	10	17–24	0.29	0.28(2)	0.214
Et==	11		0.36		0.207
Et==Λ-Rh	11	20–27	0.28	0.21(2)	0.232
Et==Δ-Rh	11	20–27	0.27	0.24(1)	0.232
Et==	12		0.37		0.222
Et==Λ-Rh	12	23–30	0.31	0.16(2)	0.238
Et==Δ-Rh	12	23–30	0.30	0.19(3)	0.239
Et==	13		0.35		0.234
Et==Λ-Rh	13	26–33	0.31	0.11(1)	0.246
Et==Δ-Rh	13	26–33	0.30	0.14(1)	0.246
Et==	14		0.38		0.212
Et==Λ-Rh	14	29–36	0.35	0.08(3)	0.221
Et==Δ-Rh	14	29–36	0.35	0.07(3)	0.221

^a See Figure 2 for calculation of donor–acceptor separations.

^b Steady-state fluorescence intensity (I_{ss}) relative to 10 μ M Ru(bpy)₃²⁺ (λ_{exc} = 480 nm, 20 °C, 5 mM phosphate, 50 mM NaCl, pH 7). ^c Fraction quenched (F_q = 1 – ($I_{Et/Rh}/I_{Et}$)) calculated from two to five sets of independent samples from different syntheses of Et/Rh conjugates; approximate errors are listed in parentheses. ^d Steady-state fluorescence polarization (P) data collected at 20 °C (see Figure 3); approximate error in polarization values = ± 0.005 .

duplexes, thus the donor/acceptor distance changes only by 3.4 Å for each base pair added to the duplex.

Thermal Denaturation Experiments. Thermal denaturation experiments monitored by UV–vis absorbance were performed on all modified assemblies. For all of the duplexes in the series, stabilization of the melting temperatures (T_m) was observed upon the incorporation of the intercalators into the duplexes. For example, in an unmodified 10 base pair duplex, T_m = 32 °C under the conditions utilized in the quenching experiments. The T_m for the corresponding Et-modified duplex is 34 °C, and for the Et/L-Rh duplex, T_m = 39 °C. The degree of stabilization observed in the 10-mer is typical for the series and the melting temperatures also increase with of duplex length, as expected. In all cases, $T_m(\text{Et/Rh}) > T_m(\text{Et-only}) > T_m(\text{unmodified duplex})$. These data demonstrate the helix stabilization which would be expected upon intercalation of the tethered moiety,⁵¹ as the observed T_m enhancements are comparable to those observed with noncovalently bound intercalators.

Steady-State Fluorescence Polarization Measurements. The Et/Rh assemblies were also characterized with respect to the intercalation environment of the donor using steady-state fluorescence polarization measurements. Measurable increases in polarization were observed upon hybridization of an ethidium-modified conjugate either to an unmodified or Rh-derivatized complement (Table 1). The observation of comparable polarizations for Et- and Et/Rh-modified duplexes confirms that the donor remains tightly intercalated upon the incorporation of the acceptor into the duplex. The maximum polarization is observed at a ratio of 1:1 Et/Rh strands (Figure 3A), confirming that the correct stoichiometries of the donor- and acceptor-modified strands are present. Duplexes of different lengths showed similar behavior. Titration of Et-modified sequences with 1–1.6 equiv of Rh-modified conjugates did not cause further increases in polarization or quenching yields, thus it appears that single-stranded Rh-conjugates do not bind to hybridized duplexes.

Temperature and viscosity-dependent polarization studies allow the determination of the duplex volume (Figure 3B).^{52,53} For this calculation, linear regression of data obtained at 20 °C

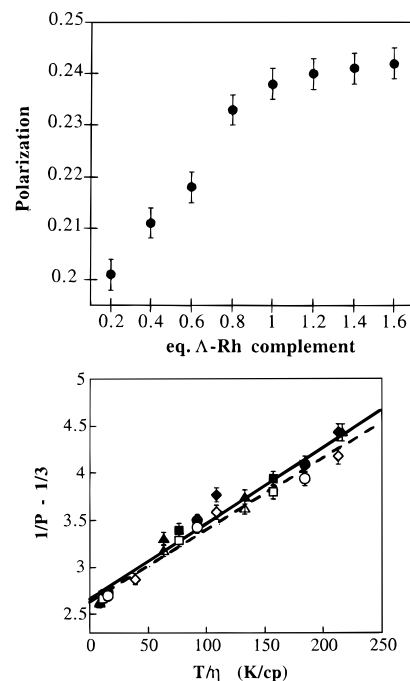


Figure 3. Steady-state fluorescence polarization assays for the structural integrity of Et/Rh-modified duplexes. (A) Fluorescence polarization as a function of hybridization for Et/Λ-Rh-12 mer. Et-strand (5 μ M) was hybridized with varying amounts of Rh-modified complement. (B) Determination of duplex volume from viscosity (η) and temperature (T) dependence of polarization (P) for Et-modified (solid line) and Et/Rh-modified (dotted line) 11-mer. The polarizations of Et and Et/Rh-modified duplexes in 0, 15, 30, and 45% sucrose in 5 mM phosphate, 50 mM NaCl, pH 7 were measured at temperatures ranging from 10–25 °C in 5 degree intervals. At temperatures approaching the melting range of the duplexes, polarization profiles were markedly nonlinear.

was utilized along with excited state lifetimes obtained by TCSPC or calculated from relative steady-state fluorescence intensities. From these measurements, volumes of $2.1(2) \times 10^4$ Å³ and $2.3(2) \times 10^4$ Å³ are obtained for the Et- and Et/Rh-modified 11-mer duplexes, respectively, which correlate closely with the calculated volumes of 2.14×10^4 Å³ and 2.32×10^4 Å³.^{54,55} Moreover, very similar temperature and viscosity profiles are observed for both duplexes; the values of P_0 , the limiting polarization, obtained in these studies can be compared and the difference in angular freedom allowed by both duplexes calculated.⁵³ This analysis also confirms that intercalated ethidium is rigidly held in both the Et-modified and the Et/Rh-modified duplex. In fact, the fluorophore actually experiences less angular freedom (average angle $\approx 3^\circ$) in the Et/Rh assembly.

Photoinduced Electron Transfer in Et/Rh Duplexes. Quenching as a Function of Duplex Length. Photoinduced electron transfer between ethidium and Rh(phi)₂bpy³⁺ in the modified duplexes was studied by steady-state and time-resolved fluorescence measurements (Table 1). The steady-state fluorescence intensities observed for the ethidium-only duplexes are essentially constant, while those for the Et/Rh systems rise with increasing distance between the two intercalators. Therefore, the amount of quenching decreases with increasing donor/

(52) Weber, G. *Biochemistry* **1952**, *51*, 145.

(53) Lakowicz, J. R. *Principles of Fluorescence Spectroscopy*; Plenum Press: New York, 1983; pp 111–153.

(54) LeBret, M. *Biopolymers* **1978**, *17*, 1939.

(55) Millar, D. P.; Roberts, R. J.; Zewail, A. H. *Proc. Natl. Acad. Sci. U.S.A.* **1980**, *77*, 5593.

(51) Saenger, W. *Principles of Nucleic Acid Structure*; Springer-Verlag: New York, 1984; and references therein.

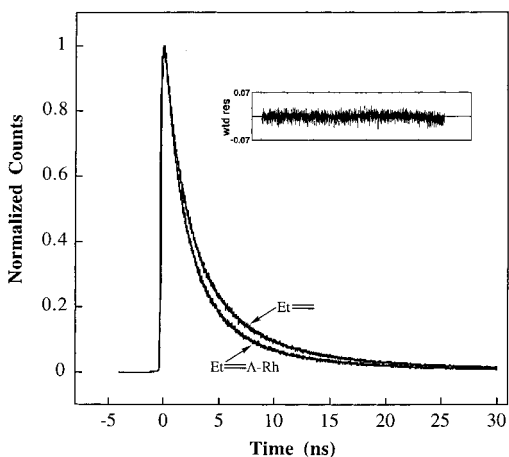


Figure 4. Normalized excited state decay profiles for Et and Et/ Δ -Rh-modified 10 base pair duplexes by TCSPC. (insert) Residuals for triexponential fit for Et/Rh 10-mer data.

acceptor separation. In a 10 base pair Et/Rh duplex, 28% of the ethidium fluorescence is quenched by the intercalated acceptor. The time scale of the quenching observed in Et/Rh duplexes was investigated using TCSPC. The excited state decay of Et' in both the unquenched and quenched duplexes was best fit to a triexponential. For example, in the Et-modified 10-mer $\tau_1 = 7.6$ ns (28%), $\tau_2 = 2.4$ ns (59%), $\tau_3 = 1.2$ ns (13%), and in the Et/ Δ -Rh analogue $\tau_1 = 7.8$ ns (18%), $\tau_2 = 2.3$ ns (65%), $\tau_3 = 0.9$ ns (17%) (Figure 4). As these lifetimes reflect only small changes in the decay kinetics, some of the quenching observed in steady-state measurements is manifested in these TCSPC measurements as a decrease in initial intensity (static quenching).⁵⁶ Hence, substantial quenching occurs on a time scale which is fast compared to the resolution of the instrument (~ 150 ps). For all of the Et/Rh duplexes studied, small changes in the triexponential excited-state decay profiles are observed relative to the duplexes modified only with ethidium; in the quenched samples, the percentage of the long lifetime component is decreased, while the percentages of the shorter lifetimes are increased. Other fitting procedures were explored in attempts to isolate a new component corresponding to an electron-transfer rate (e.g., triexponential fit for quenched sample with fixed lifetimes obtained from biexponential fit for unquenched sample), but the triexponentials obtained for both the unquenched and quenched duplexes which contained the same lifetimes in slightly different proportions yielded the most accurate description of the decay profiles. These small changes observed for the decay kinetics may indicate some quenching on the nanosecond time scale or may reflect an apparent redistribution of excited state lifetimes owing to the selective static quenching of the longest lifetime component. The similar polarization values observed for Et and Et/Rh-modified duplexes also support static quenching as the deactivation mechanism, for if larger changes in the excited state lifetimes were responsible for the observed quenching, greater changes in the polarization values would be apparent.

(56) By comparing time-resolved data to steady-state measurements or by quantitating the buildup of counts in the initial data channel by TCSPC for a fixed period of data collection, a substantial static component is present for the Et/Rh duplexes relative to the Et-duplex. The amount of static quenching approximated from these data exhibits the same variation with distance as the overall quenching, measured by steady-state methods. However, since these time-resolved data were obtained on single samples of a given duplex length rather than a sample population as in the steady-state experiments, sample variability is not accounted for in the values obtained from TCSPC, and the uncertainty in this emission intensity estimation is large. Therefore, it is more instructive to consider distance trends based upon the overall quenching observed in steady-state measurements.

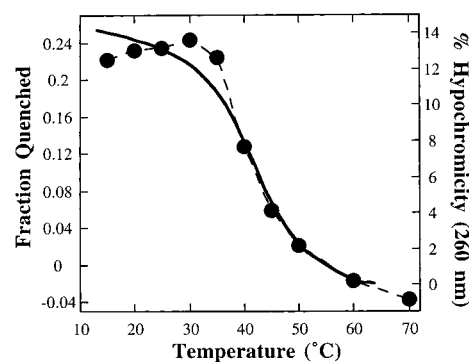
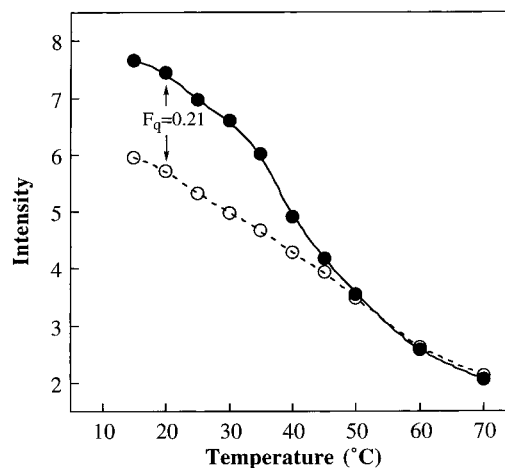


Figure 5. Temperature effects. (A) Temperature dependence of emission for the Et (filled circles) and Et/Rh-modified (empty circles) 11mer. (B) Comparison of quenching yield (circles, dotted line) and % hypochromicity (solid line).

The observed static quenching is consistent with fast electron transfer ($k \gtrsim 10^{10} \text{ s}^{-1}$) in these modified duplexes, and photoinduced quenching on this time scale parallels that observed with metallointercalators.^{4,7-9} However, this ultrafast quenching does not permit measurements of forward rates of reaction. The multiexponential decays observed in this system warrants a focus on steady-state measurements which can be more accurately analyzed. Thus, the yield of electron transfer can be quantitated by fluorescence quenching and used to evaluate the distance dependence of electron-transfer efficiency. These data offer the first examination of how the yield of an electron-transfer reaction in DNA varies as a function of intercalator donor-acceptor distance.

In order to establish that the quenching was intrahelix and not the result of factors outside the π -stack, solution conditions were varied in experiments utilizing the 11 base pair assemblies. In D_2O , where the excited state lifetime of the fluorophore is increased,⁵⁷ no decreases in quenching were observed as might be expected for a solvent-mediated process or displacement of the donor from the base stack. Additionally, only very small decreases in quenching yield occurred with increased viscosity ($\eta = 3.2$ cp) or ionic strength (10–200 mM NaCl). Investigations of the concentration dependence of the reaction revealed that the quenching yields were constant over the concentration range of 2–20 μM . At concentrations of donor-only duplexes above 20 μM , self-quenching of ethidium fluorescence was observed, reflecting interduplex intercalation. Furthermore, in experiments where the ethidium donor and rhodium(III) acceptors were localized on separate duplexes, negligible quenching was observed at 5 μM duplex concentration, eliminating the

(57) Olmsted, J.; Kearns, D. R. *Biochemistry* **1977**, *16*, 3647.

Table 2. Quenching in Et/Rh-Modified Mismatch Duplexes^a

	I_{Et}^b	$I_{Et/Rh}$	F_q^c
Et'- ⁵ C T A T C T A T C G T G A T A G A T A G C A ⁵ - Λ -Rh	0.36	0.28	0.21
Et'- ⁵ C T A T C C A T C G T G A T A G A T A G C A ⁵ - Λ -Rh	0.35	0.34	0.04
Et'- ⁵ C T A T C G A T C G T G A T A G A T A G C A ⁵ - Λ -Rh	0.37	0.25	0.26

^a T_m values were collected for each Et and Et/Rh modified duplex at same conditions used for fluorescence quenching experiments. $Et_{TA} = 37$ °C, $Et/Rh_{TA} = 43$ °C; $Et_{CA} = 23$ °C, $Et/Rh_{CA} = 26$ °C; $Et_{GA} = 28$ °C, $Et/Rh_{GA} = 34$ °C. ^b Intensities for Et (I_{Et}) and Et/Rh-modified ($I_{Et/Rh}$) duplexes are listed relative to 10 μ M Ru(bpy)₃²⁺ at 20 °C. ^c The quenching yields (F_q) at 20 °C and 10 °C were identical within error (5%).

possibility of an interduplex reaction. These results all confirm that the quenching observed in these systems is the result of an intrahelix process and therefore must proceed over extended distances mediated by the DNA π -stack.

Quenching as a Function of Base Pair Destacking. The sensitivity of the long-range quenching reaction to base-pair stacking was also examined. Figure 5A depicts steady-state fluorescence intensity of the covalently-bound fluorophore as a function of temperature for Et-modified and Et/Rh-modified duplexes. Over the temperature range where the duplex melts, the quenching is lost. Importantly, just as the melting process is reversible, the quenching loss is also reversible. When temperature-dependent quenching yields are directly compared to the loss in hypochromicity associated with base stacking (Figure 5B), it is apparent that the two phenomena are affected identically by the uncoupling of the bases at elevated temperatures. Therefore, the quenching must be occurring across a fully base-paired duplex. It is clear that the π -stack of the double helix, which is tightly stacked only in the helical form, electronically couples the acceptor and donor brought together by the complementary strands to which they are tethered.

The sensitivity of the quenching to base stacking is best illustrated in modified duplexes containing intervening mismatches. In order to maintain a constant donor-acceptor distance while perturbing stacking within the DNA helix at a constant temperature, single-base pair mismatches were introduced into 11 base pair Et/Rh-modified duplexes. Both GA and CA mismatches were incorporated into modified duplexes; NMR and crystallographic studies indicate that CA mispairs significantly perturb the stacked bases, while GA mismatches stack favorably.^{58,59} Consistent with the expected perturbations to the π -stack, the CA mismatch leads to a significant decrease in the quenching yield (Table 2). However, with a GA mismatch, the quenching reaction is as efficient as in the fully Watson-Crick base-paired duplex. These results highlight the sensitivity of DNA-mediated electron transfer to perturbations in stacking and base-pair stability within the DNA helix.

Discussion

Photoinduced electron transfer between ethidium and Rh(phi)₂bpy³⁺ bound to DNA by intercalation occurs efficiently and on a fast time scale. Fluorescence quenching of DNA-bound ethidium by rhodium is primarily static on the nanosecond time scale, and 50% quenching is apparent at low intercalator/DNA loadings (1 Et/2 Rh/50 bp). As with metallointercalators,^{4,7-9} photoinduced quenching occurs on a fast time scale ($k \geq 10^{10}$ s⁻¹). The efficiency of the electron-transfer reaction between ethidium and Rh(phi)₂bpy³⁺ is notably lower than that observed with Ru(phen)₂dppz²⁺ (dppz = dipyrldophenazine) as

a donor, despite a comparable driving force. However, the fast time scale of the quenching observed with ethidium parallels that observed with Ru(phen)₂dppz²⁺. Interestingly, when this organic heterocycle is intercalated, only the phenyl ring is exposed to the minor groove, and thus, ethidium would be less likely to participate in the clustering interactions previously proposed to facilitate fast electron transfer between metallointercalators.^{30,31} It is also noteworthy that the fast quenching observed in the Et/Rh(III) system contrasts that observed with DAP, possibly owing to the weaker intercalative binding of this acceptor.^{10,60} The different trends observed in these studies indicate that the coupling of donor-acceptor pairs into the DNA π -stack is extremely sensitive to the binding properties of the reactants.

DNA oligonucleotide duplexes containing covalently bound ethidium and rhodium intercalators were prepared in order to probe further the characteristics of photoinduced electron transfer mediated by the DNA helix. Measurements of fluorescence quenching in these modified duplexes allow the examination of the fast quenching reaction between ethidium and Rh(phi)₂bpy³⁺ without the possibility of intercalator clustering. Moreover, by systematically varying the length of the oligonucleotide region between the intercalators, we could, for the first time, examine how such photoinduced quenching varies as a function of distance separating the bound donor and acceptor.

Photoinduced electron transfer is also apparent between intercalated ethidium and rhodium in these covalently modified oligonucleotide duplexes. In DNA duplexes with ethidium and rhodium separated by ~ 20 Å, 30% of the ethidium fluorescence is quenched, while with a separation of ~ 30 Å, 10% quenching is observed. Time-resolved measurements on the modified oligomers reveal multiexponential decays of ethidium emission in the presence and absence of covalently bound rhodium and demonstrate that quenching by the rhodium complex at a pronounced donor/acceptor separation is also primarily static on the nanosecond time scale. The amount of quenching observed across the family of modified oligomers shows a shallow dependence on distance. However, the quenching yield is found to be extremely sensitive to base stacking, as is most dramatically evident in comparing quenching in modified duplexes with or without a single intervening DNA mismatch. These results all support the notion that the stacked DNA bases can facilitate long-range electron transfer.

Alternate Interpretations Considered. Given the striking difference suggested by these data in the distance dependence for electron transfer with DNA as a medium compared to proteins,⁶¹ it is important to consider first whether alternate structural models might account for these results. It is essential that the integrity of intercalation and of the duplex structures be firmly established for the results presented to be interpreted as long-range electron transfer through the base stack of DNA.

For the electron-transfer reaction to take place through the base stack in this system, both donor and acceptor must be intercalated within the DNA helix. Thermal denaturation studies demonstrate the increased helix stability of duplexes modified with each intercalator; modification with both intercalators yields still greater stabilization. The fluorescence enhancement seen for ethidium tethered to the DNA duplex compared to free

(58) Patel, D. J.; Kozlowski, S. A.; Ikuta, S.; Itakura, K *FASEB* **1984**, *11*, 2664.

(59) Brown, T.; Hunter, W. N.; Kneale, G.; Kennard, O. *Proc. Natl. Acad. Sci. U.S.A.* **1986**, *83*, 2402.

(60) Brun, A. M.; Harriman, A. *J. Am. Chem. Soc.* **1991**, *113*, 8153.

(61) Bowler, B. E.; Raphael, A. L.; Gray, H. B. *Prog. Inorg. Chem.* **1990**, *38*, 259

ethidium also is fully consistent with intercalation.³³ Fluorescence polarization data indicate that the bound ethidium is rigidly positioned. In addition, direct strand photocleavage, as found in tethered rhodium duplexes,¹ is observed only with tight intercalation of the complex,³⁴ and this photocleavage chemistry points to a pattern of intercalation sites expected based upon model building.

Might intercalation of the rhodium in DNA duplexes promote fluorescence quenching resulting from the displacement of ethidium? The higher melting temperature found for the doubly-modified duplexes is inconsistent with this notion of displacement. In addition, volumes for the DNA duplexes determined from fluorescence depolarization measurements are fully consistent with intercalation of both rhodium and ethidium (leading to the increase in length of the cylinder); indeed these data suggest greater rigidity for ethidium in the presence of rhodium. Moreover, as the lifetime of Et' in H₂O ($\tau = 440$ ps) is significantly enhanced upon intercalation ($\tau_1 = 7.6$ ns (28%), $\tau_2 = 2.4$ ns (59%), $\tau_3 = 1.2$ ns (13%)), the presence of free fluorophore either in the Et or Et/Rh modified duplex could be monitored in single photon counting experiments; no emission lifetime characteristic of the free fluorophore is detected at the concentrations under which these experiments were performed. Lastly, if the presence of bound rhodium led to apparent fluorescence quenching by making ethidium more accessible to solvent, quenching should be decreased in D₂O,⁵⁷ but in this system, the nature of the solvent has little effect on the quenching observed.

The possibility that some deformation or fraying of the duplex could lead to direct contact between the donor and acceptor may also be considered. Again, time-resolved measurements show no indication of free, nonintercalated ethidium. Polarization results rule out a gross structural heterogeneity in the duplexes, as trends observed obey relationships predicted for ellipsoid molecules of one discrete structure.⁵² While polarization measurements examine only unquenched material, these data correlate with melting studies monitored by absorbance, which also indicate structurally homogeneous duplex populations. Certainly for the shorter duplexes, where 25–30% quenching occurs, such heterogeneity in structure would be discernible by these techniques. Importantly, hypochromism as a function of temperature is found to correlate directly with fluorescence quenching, supporting the idea that the quenched population is not structurally distinctive. Moreover, similar percentages of hypochromism are observed in all the duplexes, indicating that analogous duplex structures are present in all of the Et and Et/Rh assemblies utilized in this study. One might also consider that if fraying were responsible for the observed quenching, larger amounts of quenching would be expected at elevated temperatures, where such fraying would be favored. On the contrary, the quenching observed in this system exhibits the same temperature dependence as the melting of the duplex, indicating that the loss of the well-ordered base stack eliminates the pathway for electron transfer.

The effect of an intervening CA mismatch on the quenching yield in the modified duplexes is perhaps the strongest single observation in support of a DNA-mediated reaction. If fraying at the ends were to arise, leading to some direct contact between donor and acceptor, this fraying should also occur in the DNA duplex containing the CA mismatch, yet no quenching in the duplex containing the intervening mismatch occurs. Indeed, since the mismatch-containing oligomer is less stable than that without the mismatch, based upon arguments requiring a helix opening or bending to occur, greater opening of the duplex would be expected to facilitate more quenching in the mis-

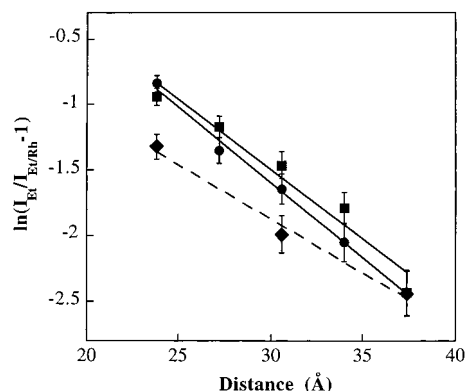


Figure 6. Distance dependence of steady-state fluorescence quenching for Et/Rh-modified duplexes. Data shown are for the Δ -Rh diastereomer with a 5'ACGA binding site (squares, long dash), Λ -Rh diastereomer with a 5'ACGA binding site (circles, solid line), and *rac*-Rh with a 5'ACAC binding site (diamonds, short dash).

matched duplex. The observation that quenching is maintained in the duplex containing the GA mismatch, which stacks well within the DNA helix, is consistent with this idea that quenching requires a well-ordered base stack. Thus, the significant loss in quenching observed with an intervening CA mismatch confirms that this reaction proceeds through the intervening base stack, not on the periphery of the helix.

Lastly, we consider whether the quenching arises through electron transfer rather than an alternate mechanism. We assign the mechanism responsible for the quenching reaction as electron transfer based primarily upon transient absorption data for ethidium and rhodium noncovalently bound to DNA. Transient absorption data provide evidence for the electron transfer products, and the yields of electron transfer intermediates, although small on the microsecond time scale, correlate with photoinduced quenching. Electron transfer between photoexcited ethidium and Rh(phi)₂bpy³⁺ is certainly thermodynamically favored ($\Delta G \sim -900$ mV). Little spectral overlap is observed between the donor emission and acceptor absorption, and hence quenching through a singlet energy transfer mechanism would be expected to be negligible. Furthermore, the dependence on distance of the quenching we observe in this system is inconsistent with either the $1/r^6$ dependence expected for a Förster mechanism or any variations on such a $1/r^6$ dependence that may arise owing to the effects of helical orientation observed previously.⁶²

Thus, data obtained in this system are fully consistent with fluorescence quenching which arises as a result of long-range electron transfer mediated by the DNA base stack. Given this electron-transfer process within the well-characterized assemblies described, the sensitivity of this reaction to distance and stacking may be examined.

Analysis of Distance Dependence. The steady-state quenching yield exhibits a logarithmic dependence on the distance separating the donor and the Rh(III) acceptor (Figure 6). If this relationship is considered within the framework of Marcus theory,⁶³ the slope of this line (0.1 \AA^{-1}) would reflect the decay of the electronic coupling with distance (β). However, time-resolved measurements of the fluorescence decay reveal that the quenching has a significant static component. Thus, these data allow us only to establish a fastest quenching rate as $\geq 10^9 \text{ s}^{-1}$ over distances varying from ~ 20 – 35 \AA . The variations in quenching observed at different donor/acceptor separations appear to be related to the *yield* of a very fast electron-transfer

(62) Clegg, R. M.; Murchie, A. I. H.; Zechel, A.; Lilley, D. M. J. *Proc. Natl. Acad. Sci. U.S.A.* **1993**, *90*, 2994.

(63) Marcus, R. A.; Sutin, N. *Biochim. Biophys. Acta* **1985**, *811*, 265.

process, rather than to a large variation in quenching rate. Qualitatively, it is apparent that DNA facilitates remarkably efficient long-range electron transfer with a shallow dependence upon distance distinct from that observed in proteins, but a meaningful value for β cannot be extracted from these data due to the fast time scale of electron transfer at all of the donor/acceptor distances investigated.

Nonetheless, the very shallow dependence of this DNA-mediated reaction on distance is inconsistent with recent theoretical studies which predict distance trends similar to those observed in proteins.²⁵ Our results indicate that the extended π -stack provides much stronger electronic coupling than observed in many protein systems, where distance dependences are dominated by σ -tunneling.⁶¹ A shallow distance dependence for the observed electron-transfer reaction might be a result of a small energetic difference between the donor excited state and the DNA bridge, in which case donor/acceptor coupling has been predicted to proceed over extended distances.^{23,64,65} However, these energies are not known. Our results underscore the need to determine experimentally the energy gaps for stacked DNA bases and species stacked within the DNA helix.

The distance dependence of this DNA-mediated electron-transfer reaction may in part reflect a structural property intrinsic to the DNA helix: stacking. It is well-known that the double helical structure of DNA is dynamic.⁵¹ Internal motions within the DNA helix have been observed on time scales ranging from milliseconds to picoseconds.^{55,66} Therefore, we propose that the quenching process is gated by disruptions in the π -stack-mediated electronic coupling; as the number of intervening base pairs increases, the probability that all base pairs will be stacked on the time scale of the electron-transfer reaction decreases.⁶⁷ Moreover, the efficiency should also depend on the stacking properties of the donor and acceptor. Thus, the quenching yield would reflect both the coupling of donor and acceptor into the helix (which remains constant with increasing duplex length) and the probability of base pair stacking (which varies exponentially with the number of intervening DNA base pairs). Such a model may explain differences in quenching seen with donors and acceptors which stack differently between the DNA base pairs. The striking correlation between quenching yields and the loss of hypochromism through the thermal activation of base pair opening indicates that the electron transfer requires a well-ordered π -stack. The sensitivity of quenching to a CA mismatch, which has a higher destacking probability, also indicates that how well the base pairs are stacked affects electronic coupling between donor and acceptor. Taken together, these findings all suggest that the probability of an electron-transfer event mediated by the DNA π -stack is modulated in part by stacking, and, thus, electron-transfer may be a sensitive reporter of base stacking.

Implications with Respect to Biological Electron Transfer.

It is clear that the system described here differs significantly

(64) Reimers, J. R.; Hush, N. S. *J. Photochem. Photobiol. A: Chem.* **1994**, *82*, 31.

(65) Evenson, J. W.; Karplus, M. *Science* **1993**, *262*, 1247.

(66) Robinson, B. H.; Mailer, C.; Drobny, G. *Ann. Rev. Biophys. Biomol. Struct.* **1997**, *26*, 629.

(67) With a simple model, expressions can be derived to relate the amount of quenching (F_q) observed in the modified duplexes to the probability of full base stacking (P_{st}) which decreases with increasing number of base pairs within the duplex (n).

$$F_q = (P_{st})^n P_D P_A$$

$$\log F_q = n \log(P_{st}) + \log(P_D P_A)$$

The quenching would also depend on stacking probabilities for the donor (P_D) and acceptor (P_A). This expression predicts a logarithmic dependence of the quenching yield on the number of base pairs between donor and acceptor, and for the data obtained from this system yields $P_{st} = 0.76$.

from donor/acceptor complexes which rely on σ -bonded arrays for electronic coupling. Based on our results for intercalated donors and acceptors, it is apparent that electron transfer through DNA is not protein-like. In classic studies of protein-mediated electron transfer using donors and acceptors at fixed distances of separation, β was found to range from 0.8 to 1.4 \AA^{-1} .⁶¹ When the oxidation of guanine by stilbene was measured in a DNA hairpin, β was calculated as 0.6 \AA^{-1} for DNA-mediated electron transfer in this system. Here, in the first systematic study of DNA-mediated electron transfer between intercalators as a function of distance, we conclude that β may be much lower or that, in the tunneling energy regime investigated, the distance dependence may be more complex.^{63,68} Indeed, β may not be the sole parameter which characterizes the distance dependence of electron transfer in DNA. For example, stacking parameters, which do not appear to be a primary issue in electron-transfer pathways for folded proteins, may also influence the distance dependence we observe.

As the base stack of DNA is not a medium dominated by σ -connectivities, but instead π -mediated stacking, it is not surprising that the difference between the electronic properties of proteins and DNA arises. Conductivity is observed in π -stacks of doped solid state materials.⁶⁹⁻⁷¹ Based on this analogy, as long as the pathway for electron-transfer goes through the π -stacked base pairs of DNA, we might expect the distance dependence to be more shallow than in proteins. Moreover, the structural properties of the double helix, which are dominated by noncovalent stacking of aromatic heterocycles, must be considered in describing long-range electron transfer across DNA. From our results, it is evident that the electronic coupling provided by DNA is highly sensitive to stacking interactions within the double helix. Indeed, the sensitivity of electron transfer to stacking is dramatically illustrated by our results with single base mismatches.

The discovery of this sensitivity to stacking may also reconcile the varying efficiencies of DNA-mediated electron-transfer reactions reported for different systems.^{3,4,7,9,10,13-15} When intercalators are utilized to probe the base stack of DNA as a medium for photoinduced electron transfer, fast kinetics are observed in reactions that proceed over long distances.^{3,4,7,9} When nonintercalating probes are employed, much steeper distance dependences and slower electron transfer kinetics result.^{10,13-15,72} Just as the efficiency of long-range electron transfer in DNA is sensitive to base stacking, it is now clear that this phenomenon is also affected by stacking interactions between the DNA bases and reporter molecules. Stacking is a crucial parameter in understanding electron-transfer processes in DNA⁷² and distinguishes this medium from proteins. Stacking interactions appear to be essential in facilitating

(68) In the analysis considered, no treatment of Franck-Condon factors, which may vary with the orientation of the intercalators with respect to the helical axis, is offered. The distance dependence of this parameter may also contribute to the observed effects.

(69) Graf, D. D.; Campbell, J. P.; Young, V. J.; Miller, L. L.; Mann, K. R. *J. Am. Chem. Soc.* **1996**, *118*, 5480.

(70) Schouten, P. G.; Warman, J. M.; deHaas, M. P.; Fox, M. A.; Pan, H.-L. *Nature* **1991**, *353*, 736.

(71) Marks, T. J. *Science* **1985**, *227*, 881.

(72) In our laboratories, a wide range of electron-transfer efficiencies has been observed for DNA-bound molecules. The reactivity of intercalated species covalently bound to DNA is highly sensitive to binding site sequence effects, which indicates that the coupling of these molecules into the base stack depends upon the integrity of the stacking interactions between these units. In addition, disparate rates of electron transfer are observed between different molecules noncovalently bound to DNA *via* intercalation. In general, ultrafast electron-transfer is only observed with strong intercalators. Weaker intercalators, or molecules with mixed binding modes, tend to undergo electron transfer at much slower rates.

reactant/DNA couplings, while no analogous parameter has been implicated in modulating coupling for σ -bonded systems.

For the electron transfer between ethidium and $\text{Rh}(\text{phi})_2\text{bpy}^{3+}$, it has been demonstrated that photoinduced electron transfer is fast, modulated by the intervening π -stack, and can take place over distances of ~ 30 Å. The variety of systems in which the DNA double helix has now been shown to facilitate charge transport over long distances provides a basis for speculation concerning mechanisms existing within cells where long-range electron transfer in DNA is utilized. Intercalating redox-active drugs targeted to DNA may employ the π -stack of DNA to broaden the range of radical migration.²¹ In addition, electronic delocalization within DNA may allow base damage to be concentrated at low-energy sites where specific repair mecha-

nisms can operate efficiently. As proteins have been specifically engineered for electron-transfer processes, we might imagine that the evolution of nucleic acids also involved electronic considerations. Our findings point to the DNA π -stack as not only a carrier of genetic information but also a pathway which is conducive to charge transport.

Acknowledgment. We are grateful to NIH (GM49216) for financial support of this research. We also thank the NIH for a predoctoral traineeship to S.O.K., the NSF for a predoctoral fellowship to R.E.H., and the American Cancer Society for a postdoctoral fellowship to E.D.A.S. In addition, we thank Prof. N. J. Turro for helpful discussions.

JA9714651